DELPHI Collaboration

DELPHI 2001-068 CONF 496
5 July, 2001

Searches for Higgs Bosons in a general Two Higgs Doublet Model

Michał Bluj[a], **Maarten Boonekamp**[b], **Julia Hoffman**[a], **Piotr Zalewski**[a]
[a] Soltan Institute for Nuclear Research, Warsaw, Poland
[b] CEA, Saclay, France

Abstract

Higgs bosons produced at LEP in association with a Z boson or in pairs are searched for over a wide mass range, using analyses relying on b-quark tagging. The data set analysed covers both the LEP 1 and LEP 2 energy range. All results presented herein are preliminary.

Contributed Paper for EPS HEP 2001 (Budapest) and LP01 (Rome)

1 Introduction

Electro-weak precise measurements [1] are in perfect agreement with the Standard Model (SM). Only the Higgs particle is still missing. The limit on its mass obtained with the direct searches exceeds already 114.3 GeV [2]. This fact, however, does not exclude an existence of a light Higgs boson outside the SM.

One doublet of complex scalar fields incorporated into the Standard Model is the simplest version of the Higgs sector consistent with the experimental data. On the other hand it is well know that models with any number of doublets and singlets of scalars can maintain the agreement with the precise measurements [3]. Models with higher representations in the Higgs sector are not excluded either, provided that large correction to the parameter $\rho = m_W^2/(m_Z^2 \cos^2\theta_W)$ are avoided. For models with only doublets and singlets $\rho = 1$ is automatic. The models are further restricted by the available limits on the FCNC processes. However, to fulfil all FCNC constraints it is sufficient to require that all fermions of one type (with the same electro-weak quantum numbers) couple to only one Higgs doublet, and that charged scalars are not too light. Moreover, a recent study has shown [4] that one of the simplest extension of the SM Higgs sector, so called Type II of two-Higgs-doublet model (2HDM), fits very well the electro-weak precise measurements while providing room for one light neutral CP-even or CP-odd Higgs particle.

In the present paper we report the search for neutral Higgs bosons in the framework of 2HDM, using topologies with at least 4 b-quarks. We take into account data collected by the DELPHI experiment both at LEP 1 and LEP 2. The results of the search in the framework of Minimal Supersymmetric Standard Model and of the so called flavour blind search can be found elsewhere [2].

1.1 Two Higgs doublet model

Many detailed descriptions of the 2HDM exist (for example [3]). Here we merely recall its main features.

In any (CP conserving) two-Higgs-doublet model, the Higgs boson spectrum consists of two CP-even Higgs bosons h^0 and H^0, a CP-odd A^0 and a pair of charged scalars H^+ and H^-. In this paper a non-supersymmetric 2HDM model of type II is considered in which, like in the MSSM, one of the Higgs doublets couples to to down-type quarks and charged leptons, whereas the second to up-type quarks.

CP-conserving version of the model has 6 free parameters. They can be chosen to be: four Higgs boson masses, the ratio of vacuum expectation values $\tan\beta = v_2/v_1$ and the mixing angle α of the CP-even neutral Higgs bosons. When this model is embedded in the MSSM then only two parameters remain independent. [3].

1.2 Higgs Boson production mechanisms at LEP

The Higgs boson searches at LEP are based mainly on the two processes:

- the Bjorken process $e^+e^- \to Z^{(*)} \to Z^{(*)}h^0$ (Fig. 1),
- the pair production $e^+e^- \to Z^{(*)} \to A^0h^0$ (Fig. 2).

Only the first process is relevant for the Standard Model in its minimal version. The cross sections for these two processes are proportional to $\sin^2(\beta-\alpha)$ and $\cos^2(\beta-\alpha)$

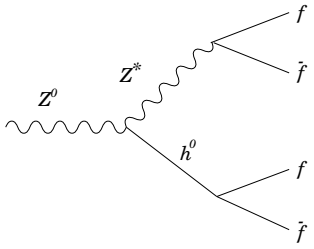

Figure 1: The Bjorken process.

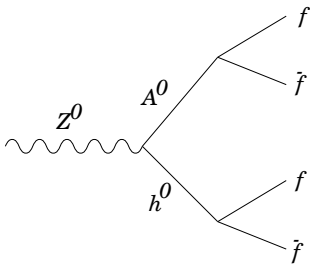

Figure 2: The pair production process.

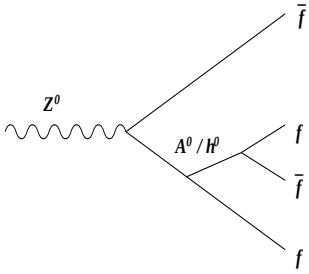

Figure 3: The Yukawa process.

respectively. The fact of non-observation of the Bjorken process, from which the mass limit for the SM Higgs boson is derived, constrains $\sin^2(\beta-\alpha)$ within the 2HDM. It can be explained in the following way. Any negative search provides a limit on the appropriate cross-section. In the case of the Standard Model the Higgs boson production rate at LEP depends only on its mass and available energy. Within models with more degrees of freedom in the Higgs sector the coupling of the h^0 boson to the Z^0 can be negligible due to mixing between scalar neutral bosons. From a recent compilation of the experimental results [4] it can be deduced that if $\sin^2(\beta-\alpha) < 0.01$ then the h^0 boson of arbitrary low mass cannot be seen via the Bjorken process in the data collected at LEP so far.

On the other hand, when $\sin^2(\beta-\alpha)$ is close to zero, then the production mechanism for the pair of Higgs bosons h^0A^0 recovers its full strength. To explain the non-observation of this process it is sufficient to assume that one of the Higgs bosons is heavy enough.

How large the mass difference can be, depends on the scenario. Within the MSSM the mass difference cannot be arbitrary large, although radiative corrections allow a significant deviation from the tree level prediction that the h^0 and A^0 bosons should be almost degenerate in mass if any of them is significantly lighter than the Z^0 boson. In the case of the 2HDM the masses of h^0 and A^0 are not related. In principle, this is true for all models not constrained by supersymmetry.

2 Analysis of the LEP 2 data

Data collected between 1998 and 2000 by the DELPHI detector with energy between 189 GeV and 208 GeV and corresponding to an integrated luminosity of 511.21 pb^{-1} were analysed (Tab. 1). For 60 pb^{-1} of the data above 205 GeV a sector known as 'S6' of the main tracking detector, the TPC, was not active. Special simulations have been made to account for the effects of this.

Large numbers of background and signal events have been produced by Monte Carlo simulation using the DELPHI detector simulation program (`DELSIM`). The size of these samples is typically more than 50 times the statistic of collected data. The background events have been generated with `PYTHIA` for QCD background ($e^+e^- \to q\bar{q}\gamma$) and `EXCALIBUR` for the four-fermion background (WW-like).

Signal simulations for different channels analysed in the present paper are described in appropriate sections.

year	1998	1999				2000c[a]	2000s[b]
E (GeV)	189	192	196	200	202	$205-208$	
$\mathcal{L}$ (pb^{-1})	158.0	25.89	76.90	84.20	41.11	164.09	61.02

[a] year 2000 energies c-processig
[b] year 2000 energies s-processig - without TPC S6 sector

Table 1: Energies and corresponding luminosities of analysed data

2.1 3-boson final states (LEP 2)

In this section we report on the search for neutral Higgs bosons decaying into lighter neutral Higgs bosons in the data collected by DELPHI detector at LEP 2.

2.1.1 Higgs boson decays to bosons

Within the general 2HDM a large mass difference between the two lightest neutral Higgs bosons is not yet experimentally excluded. Depending upon the mass hierarchy there are five new potential production and decay chains at LEP 2 (Fig. 4):

1. if $m_{h^0} > 2 \cdot m_{A^0}$ then possible channels are:
   (a) $e^+e^- \to Z^{0*} \to A^0h^0 \to A^0A^0A^0$ and
   (b) $e^+e^- \to Z^{0*} \to Z^0h^0 \to Z^0A^0A^0$
2. if $m_{h^0} > m_{Z^0} + m_{A^0}$ then possible channels are:
   (a) $e^+e^- \to Z^{0*} \to A^0h^0 \to A^0Z^0A^0$ and
   (b) $e^+e^- \to Z^{0*} \to Z^0h^0 \to Z^0Z^0A^0$
3. if $m_{A^0} > m_{Z^0} + m_{h^0}$ then possible channel is
   (a) $e^+e^- \to Z^{0*} \to h^0A^0 \to h^0Z^0h^0$

It is important to note, that above channels usually dominate if kinematically accessible. In the present note we focus on the above described production channels. We restrict our analysis to the case where the lighter neutral Higgs boson decays into b quarks and to hadronic decays of Z^0 boson. Unfortunately only channels 1a, 1b and 3a are taken into account because of the limitation of the `HZHA` generator [23], in which the other two channels are not implemented. To be more specific, the decay $h^0 \to Z^0A^0$ is not present.

2.1.2 Signal simulation

Signal events have been produced using the `HZHA` generator with the following Higgs boson masses:

1. $e^+e^- \to Z^{0*} \to A^0h^0 \to A^0A^0A^0 \to b\bar{b}b\bar{b}b\bar{b}$

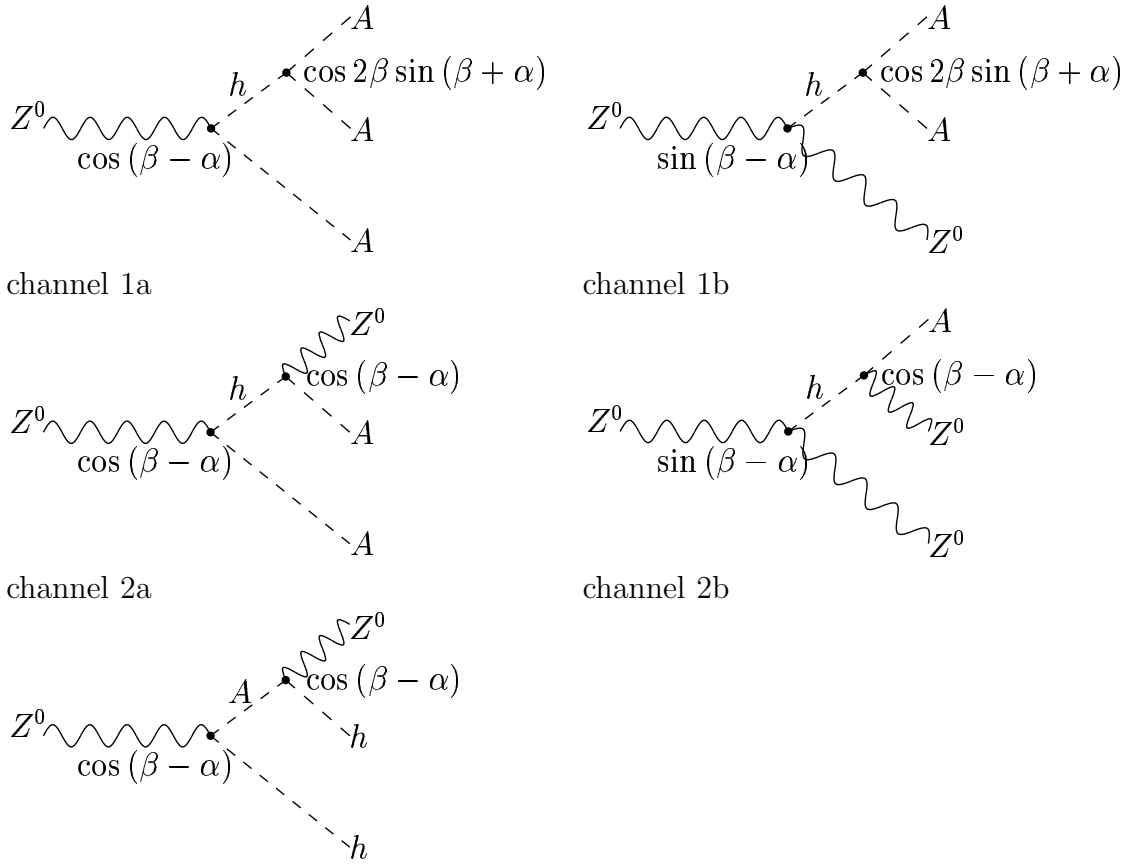

Figure 4: New production channels (see text)

$m_A = 12$ GeV $m_h = 70$, 90, 110, 130, 150, 170 GeV
$m_A = 30$ GeV $m_h = 70$, 90, 110, 130, 150 GeV
$m_A = 50$ GeV $m_h = 110$, 130 GeV

2. $e^+e^- \to Z^{0*} \to Z^0 h^0 \to Z^0 A^0 A^0 \to q\bar{q}b\bar{b}b\bar{b}$

$m_A = 12$ GeV $m_h = 30$, 50, 70, 90, 105 GeV
$m_A = 20$ GeV $m_h = 50$, 70, 90, 105 GeV
$m_A = 30$ GeV $m_h = 70$, 90, 105 GeV
$m_A = 40$ GeV $m_h = 90$, 105 GeV
$m_A = 50$ GeV $m_h = 105$ GeV

3. $e^+e^- \to Z^{0*} \to h^0 A^0 \to h^0 h^0 Z^0 \to b\bar{b}b\bar{b}q\bar{q}$

$m_h = 12$ GeV $m_A = 110$, 130, 150, 170 GeV
$m_h = 30$ GeV $m_A = 130$, 150 GeV

The size of these samples is typically 1000 events.

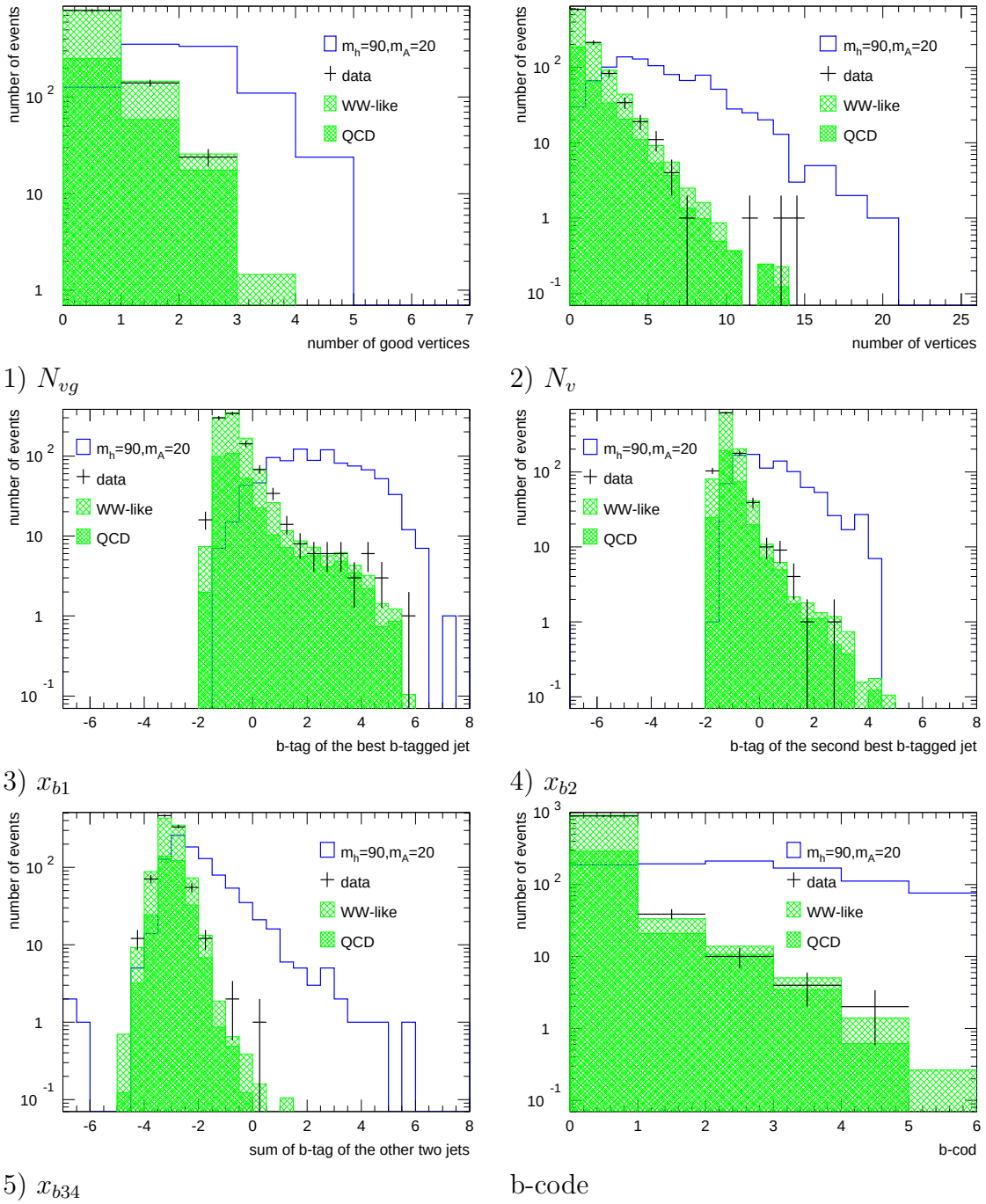

Figure 5: Data-simulation comparison for 5 variables used for b-code construction and the variable b-code itself. Empty histograms shows unnormalised distributions for one $Z^0h^0 \to Z^0A^0A^0 \to 2q4b$ signal point.

2.1.3 Signal selection method

In general one can expect a multi-jet (6-jet) topology of the signal. However, if the mass of the lighter Higgs boson only slightly exceed $2m_b$ then only 1 clear jet from the lighter Higgs boson decay can be found. This leads to a 3-jet topology in the channel with 3 lighter Higgs bosons or to 4-jet topology in the channels with Z^0 and 2 lighter Higgs bosons. This 'fusion' of two quark jets is caused by large difference between masses of the heavier and lighter Higgs bosons boosting strong the lighter Higgs bosons and by the small momentum of the primary quarks in lighter Higgs boson rest frame.

In the present analysis we are going to cover the whole kinematically allowed region of h^0, A^0 masses. It comes out that signals for some simulated points differ more among themselves than from background. Instead of elaborating each topology individually we have developed an universal method based on the fact that in each signal event there are at least $4\,b$ quarks.

Preselection used in this analysis is the standard one developed for standard Higgs boson searches in events with purely hadronic jets. It eliminates radiative and $\gamma\gamma$ events and reduces QCD background. Events are forced to four jets topology. Minimal jet mass is required do exceed 1.5 GeV. This preselection is described in detail elsewhere [2].

Since we expect at least $4\,b$-quarks in the event we use b-tagging information in a special way. Instead of the standard b-tagging we take five b-sensitive variables into account (Fig. 5):

1. number of the good secondary vertices N_{vg},
2. number of all secondary vertices N_v,
3. b-tagging of the best b-tagged jet x_{b1},
4. b-tagging of the second best b-tagged jet x_{b2},
5. b-tagging of the other two jets x_{b34}.

The new variable b-code (Fig. 5) is defined as the sum of the logical values (0, 1 for false, true respectively) of the following conditions:

$$\text{b-code} = (N_{vg} > 2) + (N_v > 5) + (x_{b1} > 2) + (x_{b2} > 0) + (x_{b34} > -2).$$

The agreement between data and simulation at the preselection level of the distributions of the variable b-code is shown in the Figure 5 and can be read from the Tables $2, 3, 4$.

2.1.4 Final efficiencies in the 3-boson final states

The results of this section are given in a form of efficiency tables $5, 6, 7$. For the final selection a cut at b-code > 3 was applied. Signal samples was generated only at energy 200 GeV. To obtain selection efficiencies corresponding to the all energies of the collected data, energy scaling was applied i.e. the four-momenta of a primary pair of bosons(hA) was rescaled to correspond to the appropriate centre-of-mass energy and then all particles coming from the primary pair were boosted accordingly. Rescaled events were analysed using the standard analysis chain.

	WW-like	QCD	data	total BKG	data/total BKG
189 GeV	1144.10	739.61	1896	1883.71	1.01
192 GeV	198.34	105.56	319	303.90	1.05
196 GeV	595.15	298.19	919	893.34	1.03
200 GeV	655.21	312.50	949	967.70	0.98
202 GeV	318.16	144.22	465	462.38	1.01
Y2K-c[a]	1295.14	563.08	1826	1858.22	0.98
Y2K-s[b]	447.48	192.06	632	639.54	0.99
all energies	4653.58	2355.21	7006	7008.79	1.00

[a] year 2000 energies c-processing
[b] year 2000 energies s-processing - without TPC S6 sector

Table 2: Agreement between data and background MC at the preselection level

	WW-like	QCD	data	total BKG	data/total BKG
189 GeV	10.79	38.41	66	49.20	1.34
192 GeV	1.75	5.99	6	7.75	0.77
196 GeV	6.75	15.69	26	22.45	1.16
200 GeV	7.22	15.63	21	22.85	0.92
202 GeV	3.37	7.56	7	10.93	0.64
Y2K-c	13.81	25.24	50	39.05	1.28
Y2K-s	5.05	8.74	14	13.79	1.02
all energies	48.75	117.26	190	166.02	1.14

Table 3: Agreement between data and background MC b-code > 1

	WW-like	QCD	data	total BKG	data/total BKG
189 GeV	1.43	1.58	2	3.01	0.66
192 GeV	0.24	0.49	2	0.73	2.73
196 GeV	1.12	1.03	2	2.14	0.93
200 GeV	1.01	1.03	2	2.04	0.98
202 GeV	0.33	0.53	1	0.85	1.18
Y2K-c	2.10	1.61	10	3.71	2.69
Y2K-s	0.61	0.60	1	1.21	0.83
all energies	6.83	6.87	20	13.70	1.46

Table 4: Agreement between data and background MC b-code > 3

mass (GeV)		# ev.	efficiencies (b-code > 3) at energy (GeV)				
m_A	m_h	gen.	198	192	196	200	206
12	70	1000	$.271 \pm .016$	$.269 \pm .016$	$.274 \pm .017$	$.273 \pm .017$	$.266 \pm .016$
12	90	999	$.442 \pm .021$	$.440 \pm .021$	$.441 \pm .021$	$.423 \pm .021$	$.418 \pm .020$
12	110	999	$.479 \pm .022$	$.481 \pm .022$	$.488 \pm .022$	$.496 \pm .022$	$.490 \pm .022$
12	130	1000	$.428 \pm .021$	$.434 \pm .021$	$.444 \pm .021$	$.441 \pm .021$	$.440 \pm .021$
12	150	993	$.363 \pm .019$	$.381 \pm .020$	$.397 \pm .020$	$.410 \pm .020$	$.424 \pm .021$
12	170	990	$.042 \pm .007$	$.046 \pm .007$	$.059 \pm .008$	$.113 \pm .011$	$.227 \pm .015$
30	70	976	$.491 \pm .022$	$.496 \pm .023$	$.485 \pm .022$	$.490 \pm .022$	$.488 \pm .022$
30	90	1007	$.525 \pm .023$	$.532 \pm .023$	$.537 \pm .023$	$.537 \pm .023$	$.537 \pm .023$
30	110	1008	$.543 \pm .023$	$.542 \pm .023$	$.544 \pm .023$	$.545 \pm .023$	$.545 \pm .023$
30	130	999	$.532 \pm .023$	$.539 \pm .023$	$.539 \pm .023$	$.537 \pm .023$	$.536 \pm .023$
30	150	982	$.501 \pm .023$	$.498 \pm .023$	$.504 \pm .023$	$.510 \pm .023$	$.510 \pm .023$
50	110	990	$.563 \pm .024$	$.569 \pm .024$	$.579 \pm .024$	$.579 \pm .024$	$.579 \pm .024$
50	130	988	$.570 \pm .024$	$.579 \pm .024$	$.584 \pm .024$	$.585 \pm .024$	$.586 \pm .024$

Table 5: Signal efficiencies in the channel $e^+e^- \to Z^{0*} \to A^0h^0 \to A^0A^0A^0$

mass (GeV)		# ev.	efficiencies (b-code > 3) at energy (GeV)				
m_A	m_h	gen.	198	192	196	200	206
12	30	999	$.069 \pm .008$	$.077 \pm .009$	$.083 \pm .009$	$.076 \pm .009$	$.083 \pm .009$
12	50	999	$.138 \pm .012$	$.138 \pm .012$	$.147 \pm .012$	$.148 \pm .012$	$.147 \pm .012$
12	70	1000	$.207 \pm .014$	$.203 \pm .014$	$.199 \pm .014$	$.198 \pm .014$	$.202 \pm .014$
12	90	1000	$.209 \pm .014$	$.218 \pm .015$	$.209 \pm .014$	$.210 \pm .014$	$.211 \pm .015$
12	105	999				$.230 \pm .015$	$.237 \pm .015$
20	50	998	$.130 \pm .011$	$.123 \pm .011$	$.122 \pm .011$	$.123 \pm .011$	$.123 \pm .011$
20	70	991	$.144 \pm .012$	$.144 \pm .012$	$.138 \pm .012$	$.138 \pm .012$	$.137 \pm .012$
20	90	997	$.190 \pm .014$	$.189 \pm .014$	$.184 \pm .014$	$.185 \pm .014$	$.184 \pm .014$
20	105	994				$.194 \pm .014$	$.211 \pm .015$
30	70	940	$.168 \pm .013$	$.170 \pm .013$	$.155 \pm .013$	$.156 \pm .013$	$.155 \pm .013$
30	90	945	$.219 \pm .015$	$.223 \pm .015$	$.222 \pm .015$	$.223 \pm .015$	$.223 \pm .015$
30	105	945				$.248 \pm .016$	$.248 \pm .016$
40	90	902	$.221 \pm .016$	$.224 \pm .016$	$.222 \pm .016$	$.223 \pm .016$	$.223 \pm .016$
40	105	901				$.261 \pm .017$	$.254 \pm .017$

Table 6: Signal efficiencies in the channel $e^+e^- \to Z^{0*} \to Z^0h^0 \to Z^0A^0A^0$

mass (GeV)		# ev.	efficiencies (b-code > 3) at energy (GeV)				
m_A	m_h	gen.	198	192	196	200	206
12	110	971	$.106 \pm .010$	$.106 \pm .010$	$.105 \pm .010$	$.106 \pm .010$	$.105 \pm .010$
12	130	970	$.146 \pm .012$	$.145 \pm .012$	$.148 \pm .012$	$.146 \pm .012$	$.154 \pm .013$
12	150	956	$.143 \pm .012$	$.141 \pm .012$	$.143 \pm .012$	$.149 \pm .012$	$.154 \pm .013$
12	170	840	$.108 \pm .011$	$.126 \pm .012$	$.135 \pm .013$	$.139 \pm .013$	$.142 \pm .013$
30	130	920	$.151 \pm .013$	$.151 \pm .013$	$.154 \pm .013$	$.157 \pm .013$	$.156 \pm .013$
30	150	917	$.158 \pm .013$	$.156 \pm .013$	$.160 \pm .013$	$.162 \pm .013$	$.162 \pm .013$

Table 7: Signal efficiencies in the channel $e^+e^- \to Z^{0*} \to h^0A^0 \to h^0Z^0h^0$

2.2 $h^0A^0 \to 4b$ at LEP 2

For the $h^0A^0 \to 4b$ channel the analysis from the previous section was directly applied. The resulting efficiency are given in the Table 8.

3 Search in $4b$ topology at LEP 1

In this section we report a search for neutral Higgs boson production at LEP 1 in $4b$ channel. The signals we are looking for are

- Yukawa production of light neutral Higgses $Z^0 \to b\bar{b}h^0(A^0) \to 4b$.
- h^0A^0 pair production without MSSM constraints;

3.1 Higgs boson production via Yukawa coupling

Preliminary analyses dealing with Yukawa Higgs boson production were sent by L3 [6] and Aleph [7] collaborations to Brussels EPS'95 and Warsaw HEP'96 conferences respectively, as well as by DELPHI collaboration [8] to Tampere EPS'99 conference. Only in the last contribution were the results concerning the $4b$ channel included.

Recently one can observe growing interest in the Yukawa Higgs boson coupling [9, 10, 11, 12] since it is one of the possible explanation of observed deviation of the muon anomalous magnetic moment from SM prediction [13]. This approach requires the existence of a light neutral Higgs particle with enhanced Yukawa couplings.

Such a particle is not excluded since it could have escaped the searches at LEP if the Higgs sector is not minimal. Even within the general two-Higgs-doublet model, an h^0 or A^0 in the energy range of LEP 1 can exist undetected. The reason is that the main two Higgs boson production mechanisms, Higgs-stralung and h^0A^0 pair production, can be suppressed or not kinematically allowed.

Such models provide two scenarios with one light CP-even or CP-odd Higgs boson:

1. the h^0 is light whereas the A^0 is heavy;
   in this case the coupling of the h^0 to the Z^0 must be small, which is equivalent to the requirement $sin^2(\beta - \alpha) \sim 0$ within the 2HDM;

mass (GeV)		# ev.	efficiencies (b-code > 3) at energy (GeV)				
m_A	m_h	gen.	198	192	196	200	206
12	50	1000	$.025 \pm .005$	$.020 \pm .004$	$.016 \pm .004$	$.013 \pm .004$	$.013 \pm .004$
12	70	999	$.157 \pm .013$	$.153 \pm .012$	$.154 \pm .012$	$.154 \pm .012$	$.145 \pm .012$
12	90	941	$.254 \pm .016$	$.250 \pm .016$	$.248 \pm .016$	$.245 \pm .016$	$.236 \pm .016$
12	110	1000	$.307 \pm .018$	$.318 \pm .018$	$.317 \pm .018$	$.314 \pm .018$	$.309 \pm .018$
12	130	1000	$.305 \pm .017$	$.311 \pm .018$	$.306 \pm .017$	$.318 \pm .018$	$.313 \pm .018$
12	150	998	$.231 \pm .015$	$.238 \pm .015$	$.242 \pm .016$	$.252 \pm .016$	$.263 \pm .016$
12	170	1000	$.086 \pm .009$	$.100 \pm .010$	$.117 \pm .011$	$.145 \pm .012$	$.171 \pm .013$
30	30	1000	$.030 \pm .005$	$.030 \pm .005$	$.029 \pm .005$	$.028 \pm .005$	$.029 \pm .005$
30	50	1000	$.160 \pm .013$	$.158 \pm .013$	$.152 \pm .012$	$.145 \pm .012$	$.141 \pm .012$
30	70	1000	$.303 \pm .017$	$.304 \pm .017$	$.308 \pm .018$	$.303 \pm .017$	$.295 \pm .017$
30	90	998	$.351 \pm .019$	$.357 \pm .019$	$.350 \pm .019$	$.352 \pm .019$	$.353 \pm .019$
30	110	1000	$.352 \pm .019$	$.356 \pm .019$	$.354 \pm .019$	$.346 \pm .019$	$.349 \pm .019$
30	130	998	$.319 \pm .018$	$.329 \pm .018$	$.337 \pm .018$	$.336 \pm .018$	$.343 \pm .019$
30	150	1000	$.240 \pm .015$	$.264 \pm .016$	$.274 \pm .017$	$.270 \pm .016$	$.272 \pm .016$
50	50	1000	$.337 \pm .018$	$.338 \pm .018$	$.337 \pm .018$	$.341 \pm .018$	$.335 \pm .018$
50	70	1000	$.331 \pm .018$	$.337 \pm .018$	$.329 \pm .018$	$.328 \pm .018$	$.334 \pm .018$
50	90	999	$.374 \pm .019$	$.379 \pm .019$	$.387 \pm .020$	$.389 \pm .020$	$.392 \pm .020$
50	110	998	$.373 \pm .019$	$.373 \pm .019$	$.375 \pm .019$	$.373 \pm .019$	$.368 \pm .019$
50	130	999	$.318 \pm .018$	$.331 \pm .018$	$.344 \pm .019$	$.338 \pm .018$	$.347 \pm .019$
70	70	999	$.368 \pm .019$	$.373 \pm .019$	$.374 \pm .019$	$.375 \pm .019$	$.379 \pm .019$
70	90	999	$.412 \pm .020$	$.415 \pm .020$	$.417 \pm .020$	$.421 \pm .021$	$.425 \pm .021$
70	110	1000	$.374 \pm .019$	$.379 \pm .019$	$.389 \pm .020$	$.383 \pm .020$	$.389 \pm .020$

Table 8: Signal efficiencies in the channel $e^+e^- \to Z^{0*} \to A^0h^0 \to b\bar{b}b\bar{b}$ at LEP2 energies

2. the A^0 is light whereas the h^0 is heavy.

In both scenarios the light neutral Higgs boson cannot be observed either via the Bjorken process or h^0A^0 pair production at LEP. However, in models with additional degrees of freedom in the Higgs sector, the Yukawa coupling of Higgs bosons to fermions can be altered. Let us consider the coupling to the down-type quarks and charged leptons within 2HDM (type II) as an example. The ratio of its strength to the strength of the corresponding coupling of the Standard Model Higgs boson ϕ^0 is given by:

a) $\sin\alpha/\cos\beta$ for the h^0 boson,

b) $\sin\beta/\cos\beta = \tan\beta$ for the A^0 boson.

The ratios are inverted for the Yukawa coupling involving the up-type quarks. An enhanced Yukawa coupling opens the possibility of a search for the Higgs boson via the third production mechanism at LEP 1, the so called Yukawa process:

- $e^+e^- \to Z^0 \to f\bar{f}h^0(A^0)$ (Fig. 3).

There are again at least two possibilities to be considered: (i) $\tan\beta \gg 1$ or (ii) $\tan\beta \ll 1$. However, an enhancement of the up-type quarks coupling in the case (ii) –

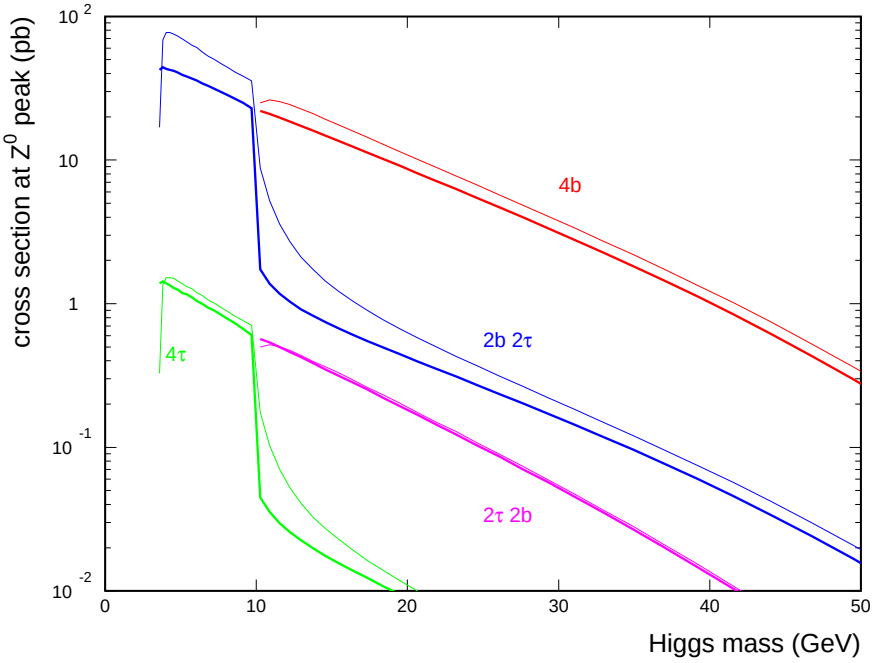

Figure 6: Higgs boson cross-sections for Yukawa process above $2m_\tau$ threshold. The thick curves shows cross-sections related to the CP-odd Higgs boson A, whereas the thin lines are drown for CP-even h^0 with $\alpha = \beta$. The cross-sections are calculated for the $\sqrt{s} =$ 91.2GeV and $\tan\beta = 30$. The differences in the production cross-sections between h^0 and A^0 are due to fermion masses properly taken into account [16], including b running mass [17].

sufficient from the production and detection point of view – is already excluded by a search for $Z \to h^0(A^0)\gamma$ process [14]. Taking this into account we will restrict our considerations to the possibility that the coupling to the down-type quarks and/or charged leptons is enhanced. It should be noted that LEP 2 $e^+e^- \to f\bar{f}$ cross-sections are too low to compete with the data recorded in the vicinity of Z^0 resonance as far as Yukawa process is concerned.

The cross-sections for Yukawa Higgs boson production at LEP 1 (above $2m_\tau$ threshold) are plotted in Figure 6. One can distinguish four distinct final topologies: $2b2\tau$, $4b$, $2\tau 2b$ and 4τ.

In the present paper we are concerned only with the $4b$ channel. Previous analysis [8] was based on reinterpretation of the Delphi measurement [18] of the gluon splitting into $b\bar{b}$. Such gluon splitting present in the process $Z^0 \to b\bar{b}g$ forms an irreducible background for the search for Yukawa production of light Higgs bosons in the $4b$ topology. But at the same time a measurement of $b\bar{b}g \to 4b$ rate sets a limit on the $b\bar{b}h(A) \to 4b$ contribution. However, the working point chosen for the gluon splitting measurement is not optimal for the search.

In the present analysis we optimise the working point from the search point of view.

3.1.1 Search in the $4b$ channel

The analysis is to be applicable to both Yukawa Higgs boson production and Higgs boson pair production. For Higgs boson masses of about half of the Z^0 mass we expect a 4 jet

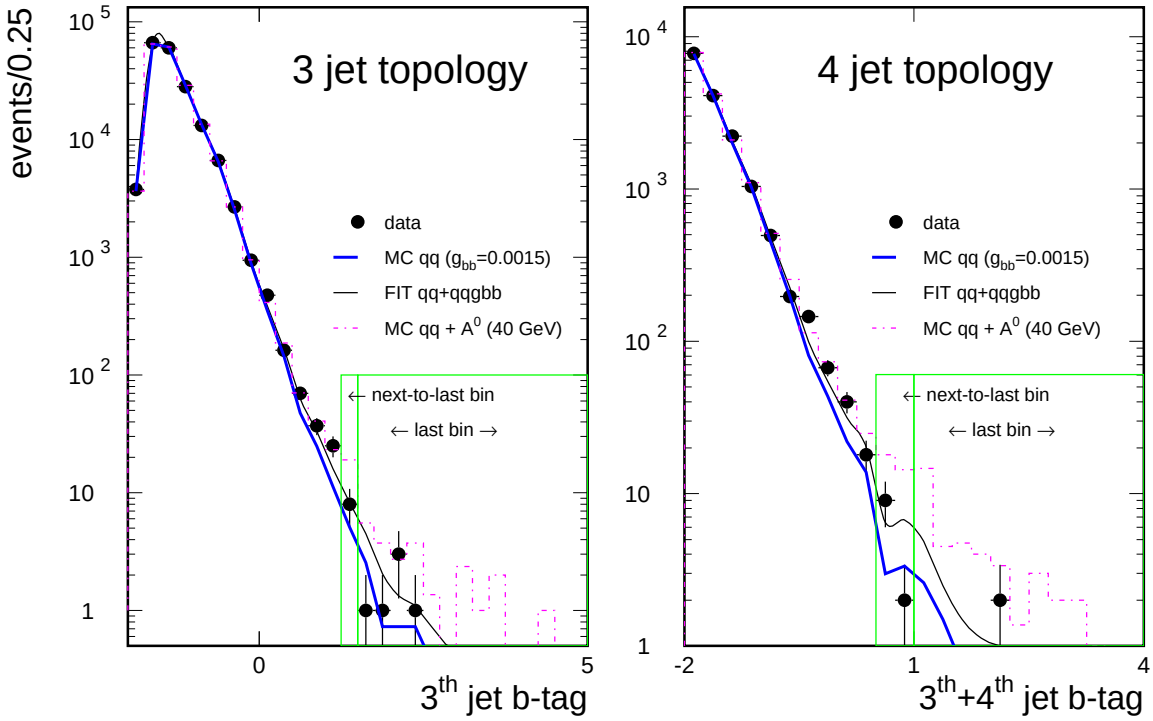

Figure 7: Data–MC agreement for two b-sensible variables taken for the present analysis.

topology, whereas in points where the mass of one of the $b\bar{b}$ pair is close to the $2m_b$ threshold the topology will be closer to 3 jets or even 2 jets. Taking this into account we develop two selections. In the first we force events to a 3 jet topology whereas in the second a 4 jet topology is used. At a given search point the selection giving better performance is taken into account.

At the preselection level we require:

- at least 6 charged particles in the event;
- Durham [19] algorithm $2 \to 3$ jets splitting greater than 0.01;
- b-tagging of the best b-tagged jet after forcing to 3 jet topology greater than 0.

Preselection eliminates all backgrounds but hadronic Z^0 decays. Non b hadronic events are greatly reduced as well.

At the working point of almost no background the b-tagging discrimination power is contained in the least tagged jets. In the figure 7 we show the distributions of variables used for final selection. They are the b-tag of the least b-tagged jet x_{b3} for the 3 jet topology and the sum of b-tags of the two least b-tagged jests x_{b34} for the 4 jet topology.

In the plots we show a fit $q\bar{q}$ and $qqg \to b\bar{b}b\bar{b}$ contributions to the data recorded in the years 1994 and 1995. As can be seen the fit suggest an additional $qqg \to b\bar{b}b\bar{b}$ contribution in agreement with the previous Delphi measurement [18].

To be conservative we do not take into account this additional contribution of $b\bar{b}g \to 4b$ events. For derivation of limits we take only expectation based on the standard Delphi

$q\bar{q}$ MC (thick lines in the Fig 7) in which $g_{b\bar{b}} = 1.5 \cdot 10^{-3}$. This value is about factor 2 lower than current world $g_{b\bar{b}}$ average. It is also lower than central value of the theoretical evaluation (accurate to the leading order in α_s, and with resummation of large leading and next-to-leading logarithmic terms to all orders) which gives $g_{b\bar{b}} = 1.8^{+0.4}_{-0.5} \cdot 10^{-3}$ [20].

In the figure 7 we show also "bins" taken for the final analysis. They were chosen to have similar number of expected MC $q\bar{q}$ events and at least 1% to 2% efficiency in the "last bin" for signal points. Numbers of expected and found events in the defined bins are the following:

			MC $q\bar{q}$	data (94-95)
3 jet topology:	the last bin	$x_{b3} > 1.5$	5.5	6
4 jet topology:	the last bin	$x_{b34} > 1.0$	5.5	2
3 jet topology:	the next-to-last bin	$1.25 < x_{b3} < 1.5$	4.7	8
4 jet topology:	the next-to-last bin	$0.5 < x_{b34} < 1.0$	5.7	11

To be conservative, we do not profit from the deficit in the last bin of 4 jet topology. For each bin (the last and next-to-last) we take the worst case of 3 jet and 4 jet topologies, namely 5.5 expected, 6 events found events for the last bin and 5.7 expected, 11 events found for the next-to-last bin.

3.1.2 Final analysis of the Yukawa Higgs boson production in the $4b$ channel

About 10000 $e^+e^- \to b\bar{b}h^0(A^0)$ events were generated with a generator based on ref. [16, 17]. The events were subsequently hadronized with JETSET 7.3 [21] and introduced to the detailed simulation of the DELPHI detector using DELSIM program [22].

Efficiencies for both h^0 and A^0 are shown in the figure 8. Only for small Higgs boson masses does the 3 jet topology perform better than the 4 jet one. The 4 jet topology is always better in the next-to-last bin (3 jet efficiencies are not shown for this bin).

The curves shown in the figures are taken as the estimates of the efficiency dependence on the Higgs boson mass. They are fitted with 3^{th} order polynomials. The shape of the dependence is easy to understand. In the 3 jet topology very good b-tagging can be obtained if a good Higgs$\to b\bar{b}$ jet is present in the event, which is probable for Higgs boson masses close to the $2m_b$ threshold, or if at least one of the jets from the Higgs boson decay is well isolated, which is possible for larger Higgs boson masses. The latter situation is needed for higher efficiency in the 4 jet topology. The decrease of the efficiencies for Higgs boson masses close to the Z^0 mass is caused by smaller and smaller energy available for jets produced at Z^0 decay.

The final results shown in the figure 9 were obtained combining the next-to-last bin (5.7 expected 11 events found) and the last bins (5.5 expected 6 events found) as independent measurements. For the last bin the maximum of 3 jet and 4 jet topologies was taken. For this preliminary results systematic errors on the efficiency have not been allowed for.

The use of next-to-last bin on top of the last bin improves the cross-section limit by about 10%. The last been taken alone has 95% CL limit at 7 events. This could be compared to the previous result [8] where the limit was set at 50.4 events for 4-8% efficiency. The improvement in the cross-section limit is about 3 fold.

As it was stated in the section 3.1 one possible explanation for the discrepancy recently fond in the measurement of anomalous muon magnetic moment could be a contribution from the light neutral scalars from 2HDM. Whereas one-loop calculation suggested that

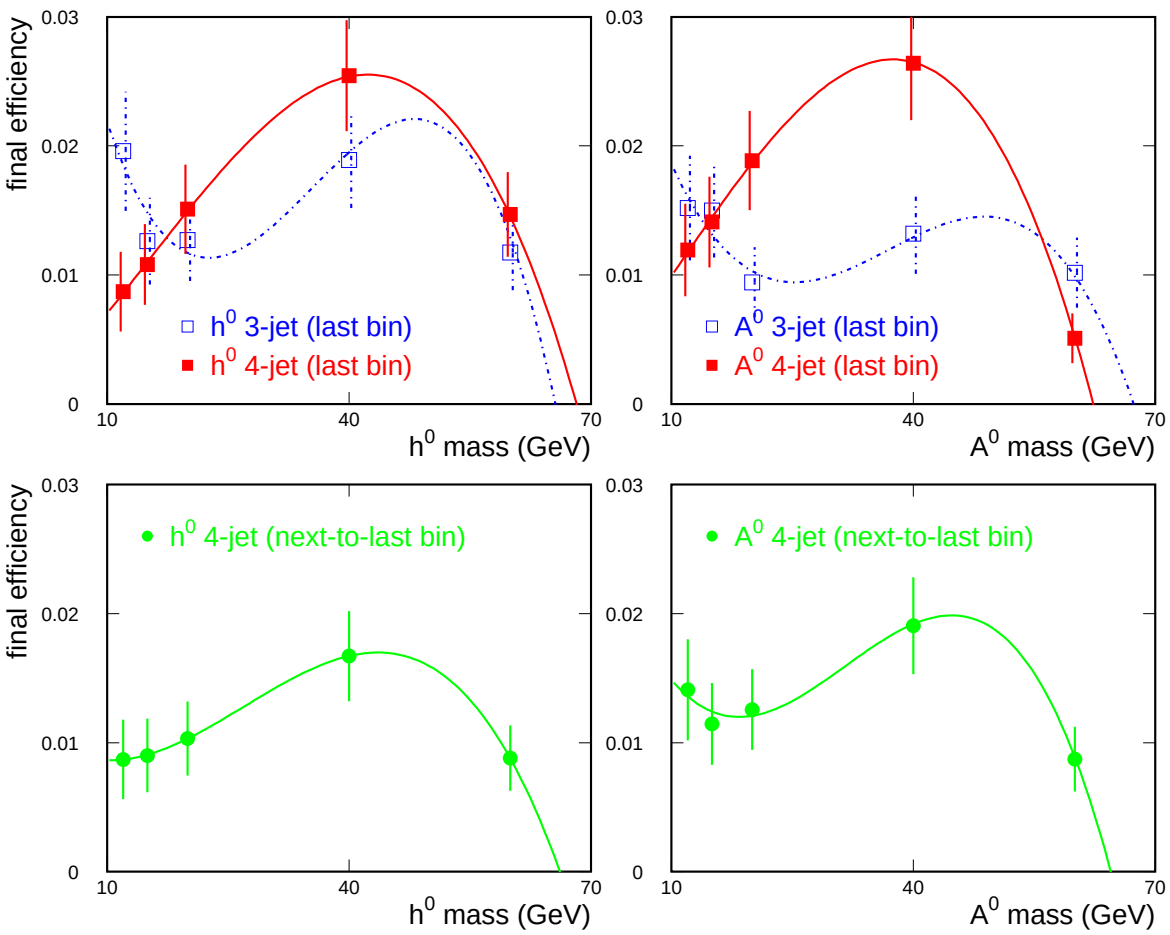

Figure 8: Final efficiencies in the $4b$ channel of the Yukawa Higgs production at LEP 1

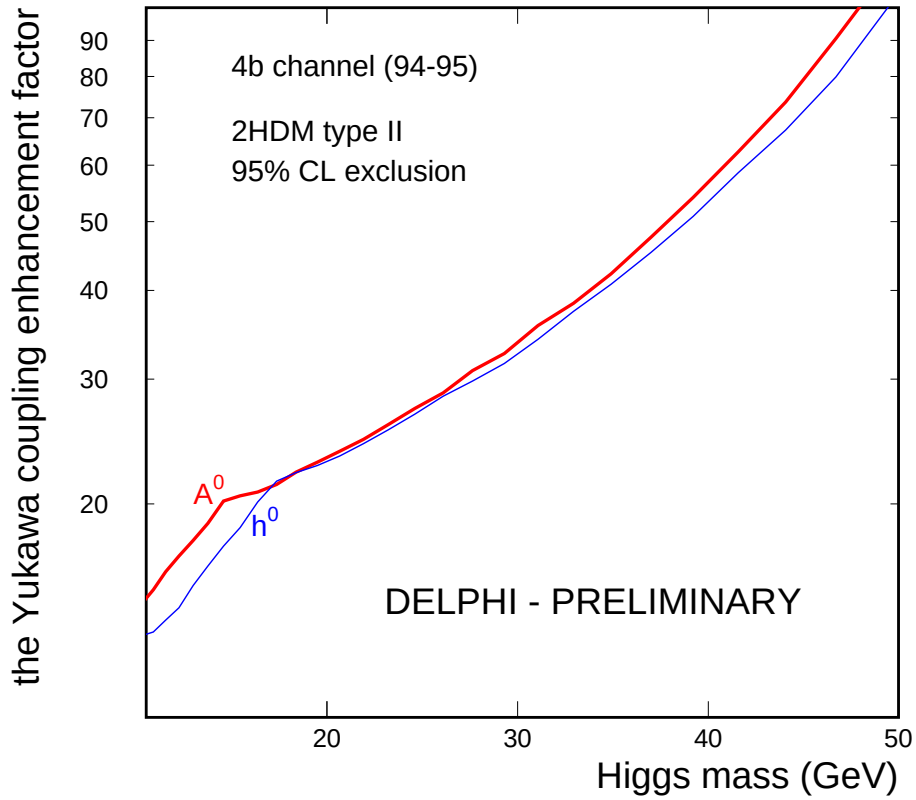

Figure 9: The exclusions within 2HDM type II in $4b$ channel. The enhancement factor shown in the vertical axis corresponds to $\tan\beta$ and $\sin\alpha/\cos\beta$ for A^0 and h^0 respectively.

light h^0 should be taken into account [9, 10], the two-loop contribution changes the situation completely [15, 11, 12]. Now the presence of light A^0 can explain the discrepancy. The change comes from the fact, that at 2-loop level a Higgs boson could connect a muon line with a fermion loop, reducing the number of vertices with small Higgs-muon coupling from two (at 1-loop) to one. Present analysis of DELPHI data in the $4b$ channel enables the exclusion of a substantial part of the region of $(M_{A^0}, \tan\beta)$ parameters space in which the A^0 contribution alone could explain the muon g-2 discrepancy.

3.2 Pair production at LEP1 in the $4b$ channel

The analysis developed for the Yukawa Higgs boson production was applied directly to the pair production of neutral Higgs bosons at LEP 1. Resulting efficiences are given in the Table 9. The efficiences were evaluated for both 3 jet and 4 jet selection. At the given point the method with beter efficiency in the last bin was chosen.

4 Interpretation of the results

The search for Higgs boson production with reduced cross sections (compared, for instance, to those predicted in the MSSM) are of great interest. As stated above, in the framework of the general 2HDM, the mixing angles α and β are free parameters and therefore the suppression of the Higgs boson production cross section can be large. Similarly, although a high branching fraction of the scalar and pseudoscalar Higgs bosons into a pair of b-quarks is expected since the Higgs boson tends to decay into the most heavy kinematically accessible fermion pair, mixing between the Higgs doublets may change this property and introduce an additional suppression.

Higgs boson production is tested using the results of the analyses described above. For each process, a global suppression factor is defined as the product of cross-section suppression, and branching ratio suppression. The m_h, m_A plane is then scanned and exclusion is tested for different values of this suppression factor.

Such a procedure allows a model independent approach : to see whether a given point in any specific model's parameter space is excluded it is sufficient to calculate the corresponding global suppression factor and to compare it with the excluded value.

Event rates are computed from the cross-sections calculated by HZHA generator [23] and using interpolation of the efficiencies listed in the tables given above. The combination of data at different centre-of-mass energies was done assuming usual evolution of the hA and hZ production cross-section with energy.

The Figure 10 shows the results of the present analysis in the case of h^0A^0 production and decay into four b-quarks. A strong sensitivity is obtained both at high mass from LEP 2 data, and in the lower mass region where the LEP 1 data contribute significantly. In the case of no suppression (i.e. $\cos^2(\alpha-\beta) = 1$, and 100% branching into 4b), a triangle is excluded roughly given by $m_h, m_A > 15\,\mathrm{GeV}$, and $m_h, m_A < 180$ GeV. When the suppression factor is equal to 0.1, the remaining excluded region is obtained essentially from LEP 1 data.

Another display of the excluded suppression factor is given in the Figure 11, as a function of m_h, and assuming $m_h = m_A$. Contrarily to the previously discussed figure, it was obtained from the MSSM hA search described in reference [2], which is optimized for

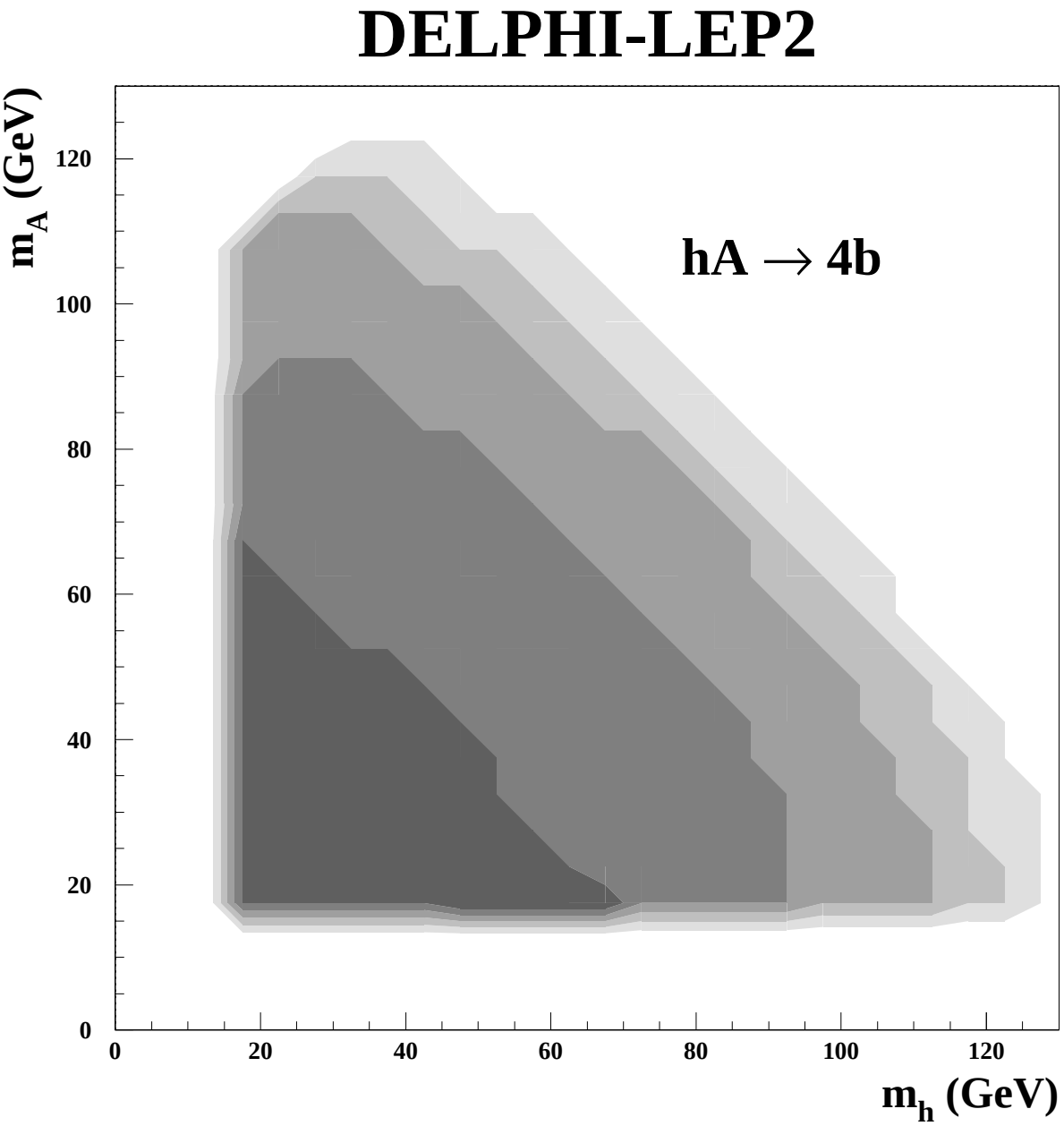

Figure 10: Region in the m_h, m_A plane where pair-production of h^0A^0 and decay into four b-quarks is excluded by the present analysis, using LEP 1 and LEP 2 data. The levels of gray correspond to suppression factors of 0.1, 0.3, 0.5, 0.75, and 1, from darker to lighter gray respectively.

mass (GeV)		# ev.	the last bin eff.		the next-to-last bin eff.	
m_A	m_h	gen.	3 jet [10^{-3}]	4 jet [10^{-3}]	3 jet [10^{-3}]	4 jet [10^{-3}]
12	12	1969	$1. \pm 1.$	$1. \pm 1.$	$1. \pm 1.$	$1. \pm 1.$
12	20	1980	$21. \pm 3.$	$4. \pm 1.$	$14. \pm 3.$	$14. \pm 3.$
12	30	1987	$20. \pm 3.$	$10. \pm 2.$	$15. \pm 3.$	$15. \pm 3.$
12	40	1983	$22. \pm 3.$	$8. \pm 2.$	$8. \pm 2.$	$16. \pm 3.$
12	50	1981	$18. \pm 3.$	$11. \pm 2.$	$13. \pm 3.$	$14. \pm 3.$
12	60	1979	$17. \pm 3.$	$8. \pm 2.$	$11. \pm 2.$	$14. \pm 3.$
12	70	1968	$6. \pm 2.$	$6. \pm 2.$	$3. \pm 1.$	$2. \pm 1.$
20	12	1989	$14. \pm 3.$	$8. \pm 2.$	$9. \pm 2.$	$8. \pm 2.$
20	20	1991	$23. \pm 3.$	$9. \pm 2.$	$30. \pm 4.$	$26. \pm 4.$
20	30	901	$26. \pm 5.$	$14. \pm 4.$	$44. \pm 7.$	$22. \pm 5.$
20	40	1429	$10. \pm 3.$	$10. \pm 3.$	$22. \pm 4.$	$18. \pm 4.$
20	50	726	$18. \pm 5.$	$10. \pm 4.$	$26. \pm 6.$	$19. \pm 5.$
20	60	1989	$10. \pm 2.$	$12. \pm 2.$	$13. \pm 3.$	$16. \pm 3.$
30	12	1984	$28. \pm 4.$	$7. \pm 2.$	$18. \pm 3.$	$17. \pm 3.$
30	20	1991	$14. \pm 3.$	$10. \pm 2.$	$33. \pm 4.$	$29. \pm 4.$
30	30	1241	$15. \pm 4.$	$4. \pm 2.$	$34. \pm 5.$	$24. \pm 4.$
30	40	1303	$11. \pm 3.$	$7. \pm 2.$	$25. \pm 4.$	$20. \pm 4.$
30	50	1814	$11. \pm 2.$	$6. \pm 2.$	$23. \pm 4.$	$13. \pm 3.$
40	12	1986	$19. \pm 3.$	$10. \pm 2.$	$16. \pm 3.$	$15. \pm 3.$
40	20	1161	$15. \pm 4.$	$6. \pm 2.$	$26. \pm 5.$	$20. \pm 4.$
40	30	1997	$14. \pm 3.$	$8. \pm 2.$	$27. \pm 4.$	$13. \pm 3.$
40	40	1463	$14. \pm 3.$	$10. \pm 3.$	$25. \pm 4.$	$18. \pm 4.$
50	12	1983	$23. \pm 3.$	$13. \pm 3.$	$13. \pm 3.$	$11. \pm 2.$
50	20	1996	$14. \pm 3.$	$10. \pm 2.$	$19. \pm 3.$	$17. \pm 3.$
50	30	1992	$11. \pm 2.$	$5. \pm 2.$	$22. \pm 3.$	$16. \pm 3.$
60	12	1991	$17. \pm 3.$	$6. \pm 2.$	$12. \pm 2.$	$9. \pm 2.$
60	20	1991	$14. \pm 3.$	$10. \pm 2.$	$17. \pm 3.$	$14. \pm 3.$
70	12	1987	$8. \pm 2.$	$6. \pm 2.$	$4. \pm 1.$	$7. \pm 2.$

Table 9: Signal efficiencies in the channel $e^+e^- \to Z^{0*} \to A^0h^0 \to b\bar{b}b\bar{b}$ at LEP1

equal masses. In this figure, LEP 2 data only are exploited and therefore the considered mass range starts at 40 GeV.

Production of four b-quarks in association with a hadronic Z^0 decay, through the process $h^0Z^0 \to A^0A^0Z^0$ is constrained in Figure 12. The covered m_h range is bounded from above because of the high mass of the associated Z^0 boson. In the case of no suppression (in other words, if this channel is dominant), the present analysis constrains the h^0 mass to be above 105 GeV. If the suppression is below 0.3, no excluded region survives.

The similar $h^0A^0 \to h^0h^0Z^0$ process was found to be unconstrained by the present work. The reasons are that the h^0A^0 cross-section decreases much faster than the h^0Z^0 cross-section when approaching the kinematic limit, leading to reduced sensitivity. Besides, the apparent excess observed in the data taken in the first period of 2000 (see Table 4), although not confirmed by the other samples, is enough to forbid any exclusion in this

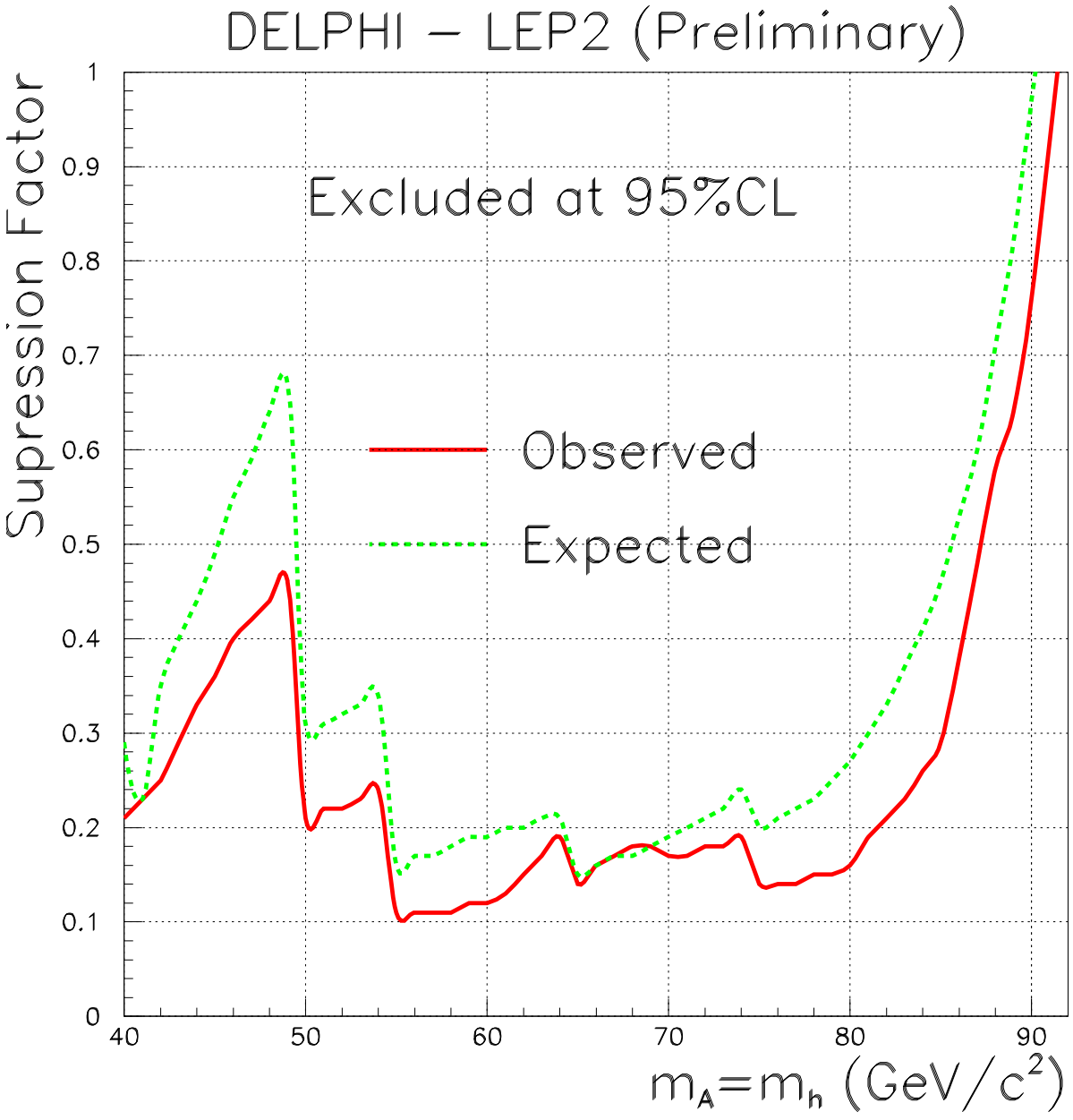

Figure 11: Excluded suppression factor, along the diagonal $m_h = m_A$, in the range 40 to 90 GeV. This result is obtained from LEP2 data only.

channel.

Finally, topologies with six b-quarks, originating from h^0A^0 with intermediary decay of the h^0 boson into two A^0 bosons, are tested in the Figure 13. The high number of b-quarks in the final state makes the search particularly sensitive, even for small suppression factors.

5 Conclusions

Relying extensively on a universal b-tagging analysis, searches for Higgs boson production have been performed in various channels, using the data recorded by DELPHI at LEP 2. The well-known $h^0A^0 \to 4b$ channel has been revisited and gained extended sensitivity towards large h^0 and A^0 mass differences. The decay $h^0 \to A^0A^0$ was also considered and searched for in h^0A^0 and h^0Z^0 production. In these three cases large portions of the $m_h - m_A$ plane are excluded as a function of global a suppression factor. The decay $A^0 \to h^0Z^0$ was also studied but found very difficult.

Four-b final states were also studied at LEP1, in the h^0A^0 channel and most importantly in the Yukawa channels. the results of the h^0A^0 channel allowed to contribute to the coverage of the $m_h - m_A$ plane at low masses. Within the 2HDM, the Yukawa search allowed to constrain tightly the enhancement of the h^0 and A^0 coupling to b-quarks for a large mass range of these bosons.

Acknowledgements

We would like to thank M. Krawczyk, J. Kalinowski for providing us with generators used for Yukawa process search, and for useful discussions

Work supported in part by Polish State Committee for Scientific Research under grants 2P03B06015, 2P03B03311 and SPUB/P03/178/98.

References

[1] Electro-Weak LEP Working Group contribution to the EPS-HEP2001 Conference, Budapest, Hungary, July 2001.

[2] DELPHI Collaboration contribution to the EPS-HEP2001 Conference, Budapest, Hungary, July 2001.

[3] J. F. Gunion, H. E. Haber, G. Kane, S. Dawson, *The Higgs Hunter's Guide*, Addison-Wesley Publishing Company.

[4] P. Chankowski, M. Krawczyk, J. Żochowski, IFT-98/20, hep-ph/9905436

[5] DELPHI Collaboration, P. Abreu *et al.*, CERN-EP/98-180 (1998).

[6] The L3 Collaboration, contributed paper 98 to the Brussels EPS Conference 1995.

[7] The ALEPH Collaboration, paper PA13-027 submitted to the *XXVIII Rochester Int. Conf, on High Energy Physics*, Warsaw, Poland, July 1996.

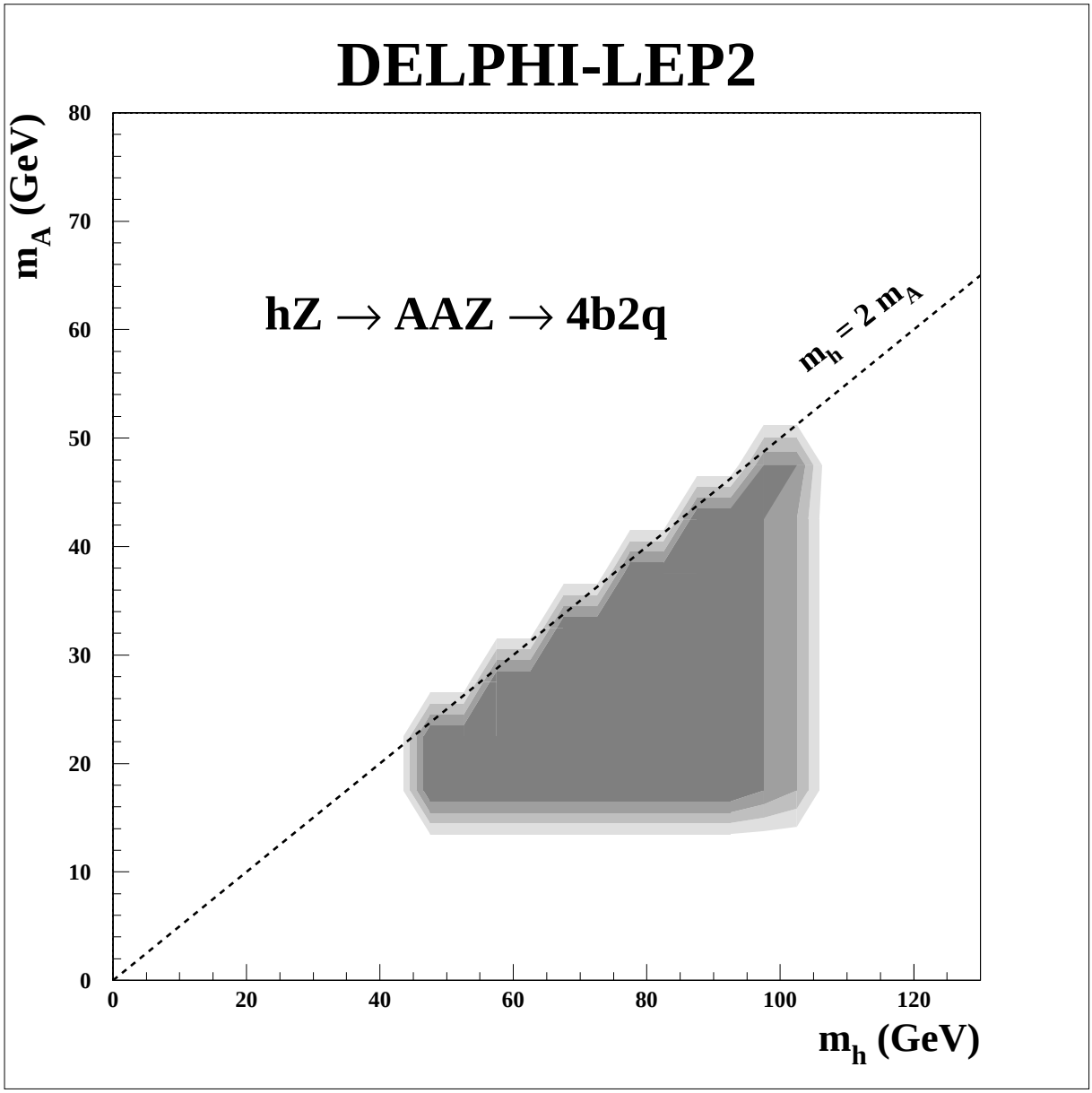

Figure 12: Region in the m_h, m_A plane where production of $h^0 Z^0$, subsequent decay of h^0 into $A^0 A^0$, and production of six quarks (at least four are b-quarks) in the final state, is excluded by the present analysis. The levels of gray correspond to suppression factors of 0.3, 0.5, 0.75, and 1, from darker to lighter gray respectively.

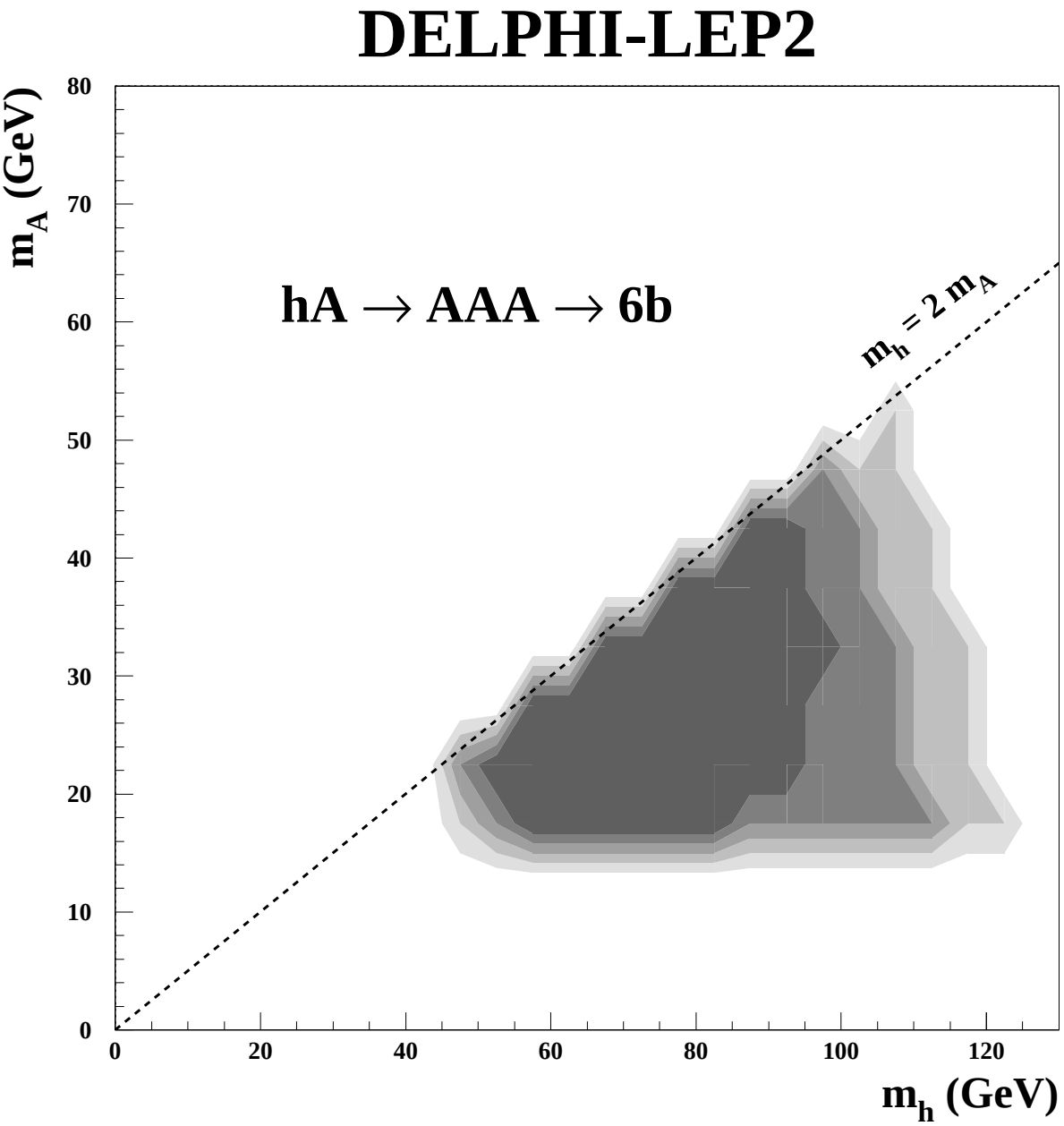

Figure 13: Region in the m_h, m_A plane where production of h^0A^0, subsequent decay of h^0 into A^0A^0, and production of six b-quarks in the final state, is excluded by the present analysis. The levels of gray correspond to suppression factors of 0.1, 0.3, 0.5, 0.75, and 1, from darker to lighter gray respectively.

[8] The DELPHI Collaboration, paper tmp-7-120 submitted to HEP'99 EPS Conference, Tampere, Finland, July 1999; DELPHI 99-76 CONF 263.

[9] A. Dedes, H. E. Howard, hep-ph/0102297 v3.

[10] M. Krawczyk, hep-ph/0103223 v2.

[11] D. Chang, We-Fu Chang, C.-H. Chou, W.-Y. Keung, hep-ph/0009292 v3

[12] K. Cheung, C.-H. Chou, O.C.W. Kong, hep-ph/0103183 v1

[13] H. N. Brown *et al.*, Muon g-2 Collaboration, hep-ex/0102017.

[14] M. Krawczyk, J. Żochowski, P. Mättig, hep-ph/9811256.

[15] M. Krawczyk, private communication.

[16] J. Kalinowski, M. Krawczyk Phys. Lett. B 361 (1995) 66.

[17] J. Kalinowski, M. Krawczyk IFT-96-03 preprint, Warsaw 1996.

[18] DELPHI Collaboration, P. Abreu *et al.*, CERN-EP/99-226 (1999).

[19] S. Catani *et al.*, Phys. Lett. **B269** (1991) 432;
N. Brown, W. J. Stirling, Z. Phys. **C53** (1992) 629.

[20] M. H. Seymour, Nucl. Phys. **B 436** (1995) 163.

[21] T. Sjöstrand et al., in *Z physics at LEP 1*, CERN 89-08, CERN, GENEVA 1989.

[22] DELPHI Collaboration, P. Abreu *et al.*, Nucl. Inst. Meth. **A378** (1996) 57.

[23] P. Janot, in CERN Report 96-01, Vol. 2, p. 309 (1996)